

# Mutations in the *pqe-1* Gene Enhance Transgene Expression in *Caenorhabditis elegans*

Koji Yamada, Jun-ichi Tsuchiya, and Yuichi Iino<sup>1</sup>

Department of Biophysics and Biochemistry, The University of Tokyo, Tokyo 113-0033, Japan

**ABSTRACT** Although various genetic tools have been developed and used as transgenes, the expression of the transgenes often is hampered by negative regulators. Disrupting such negative regulators of gene expression is potentially a way to overcome the common problem of low expression of transgenes. To find such regulators whose mutations enhance transgene expression in *Caenorhabditis elegans*, we took advantage of a newly developed reporter transgene, *lin-11pAΔ::venus*. This transgene induces expression of a fluorescent protein, Venus, in specific neurons including AIZ, where the expression was stochastic. The frequency of reporter expression in AIZ seemed to be correlated with the strength of transgene expression. By using this system, in which a moderate increase of expression was converted to all-or-none expression states, we describe here a forward genetic screen for mutations that enhance the expression of transgenes. Through the screen, we found that mutations in the *pqe-1* gene, which encodes a Q/P-rich nuclear protein with an exonuclease domain, increase the chance of reporter expression in AIZ. The fluorescence intensity in RIC, in which all *lin-11pAΔ::venus* animals show reporter expression, was increased in *pqe-1* mutants, suggesting that *pqe-1* reduces the expression level of the transgene. Expression of transgenes with other promoters, 3'UTR, or reporter genes was also enhanced by the *pqe-1* mutation, suggesting that the effect was not specific to a particular type of transgenes, whereas the effect did not seem to extend to endogenous genes. We propose that *pqe-1* mutants can be used to increase the expression of various useful transgenes.

## KEYWORDS

*Caenorhabditis elegans*  
transgene  
expression  
*pqe-1*

Various genetic tools have been developed and used for probing and manipulating molecular and cellular functions in model organisms. For example, green fluorescent protein (GFP) and related fluorescent proteins are used to visualize gene expression or dynamics of proteins (Chalfie *et al.* 1994). Calcium indicators like cameleon (Miyawaki *et al.* 1997) and GCaMP (Nakai *et al.* 2001) were derived from fluorescent proteins and used to visualize intracellular calcium responses. Recently developed optogenetic tools, such as channelrhodopsin-2 (Boyden *et al.* 2005) and halorhodopsin (Zhang *et al.* 2007), are useful for manipulating the activity of neurons. These are powerful experi-

mental tools, but it can be difficult to get them expressed in sufficient levels. Introducing transgenes in high copy numbers does not always lead to strong expression because repetitive sequences often cause gene silencing (Hsieh and Fire 2000). To increase the expression of transgenes without modifying the coded proteins, several methods could be applied. For example, optimization of codon usage within the coding sequence, by incorporating codons for the most abundant isoaccepting tRNA, is known to increase expression (Ikemura 1985). Recently, it was also reported that optimizing the codons to stabilize the mRNA around the ribosomal binding site effectively increases the gene expression in *Escherichia coli* (Kudla *et al.* 2009). In addition, refining the sequences of untranslated regions, 5'UTR and 3'UTR, or introducing synthetic introns also results in an increase of gene expression in eukaryotes by optimizing posttranscriptional processes (Le Hir *et al.* 2003; Mignone *et al.* 2002).

In the soil nematode *Caenorhabditis elegans*, transgenes injected into the germline form large heritable extrachromosomal arrays consisting of dozens to several hundreds of copies through recombination (Mello *et al.* 1991; Stinchcomb *et al.* 1985). However, these repetitive transgenes show lower expression levels than that expected from their copy numbers. This suppression is probably attributable to gene

Copyright © 2012 Yamada *et al.*

doi: 10.1534/g3.112.002832

Manuscript received March 30, 2012; accepted for publication April 24, 2012

This is an open-access article distributed under the terms of the Creative Commons Attribution Unported License (<http://creativecommons.org/licenses/by/3.0/>), which permits unrestricted use, distribution, and reproduction in any medium, provided the original work is properly cited.

Supporting information is available online at <http://www.g3journal.org/lookup/suppl/doi:10.1534/g3.112.002832/-/DC1>.

<sup>1</sup>Corresponding author: Department of Biophysics and Biochemistry, Graduate School of Science, The University of Tokyo, Science Building No.3, rm224, 2-11-16 Yayoi, Bunkyo-ku, Tokyo 113-0033, Japan. E-mail: iino@biochem.s.u-tokyo.ac.jp

silencing of repetitive sequences because less-repetitive arrays formed by co-introduction of transgenes with excess *C. elegans* genomic DNA cause greater expression (Kelly *et al.* 1997). To characterize the mechanisms of gene silencing of repetitive arrays in somatic cells, screens for mutations that enhance the silencing of fluorescent reporter genes were previously performed. In the screens, mutations in a RING finger/B-Box factor TAM-1, a retinoblastoma-like protein LIN-35, and a bromodomain protein LEX-1 were all identified to enhance the silencing in somatic cells (Hsieh *et al.* 1999; Tseng *et al.* 2007). In contrast, mutations that enhance expression of transgenes have not been reported, to the best of our knowledge. Detecting subtle increases in reporter expression would be difficult because the expression level of transgenes in individual animals is variable even in a wild-type population. Although it is challenging, if we obtain mutations that enhance the expression of transgenes generally, we will be able to apply such mutations to increase the expression of useful genetic tools.

The nervous system of *C. elegans* comprises 302 neurons, each with specialized functions (White *et al.* 1982). Among those neurons, AIZ neurons receive inputs from several sensory neurons and act in the integration of thermosensory signals (Mori and Ohshima 1995). They are also indispensable for salt chemotaxis (Iino and Yoshida 2009). In the course of characterizing the function of AIZ, we produced a composite promoter *lin-11pAΔ*, which induced fluorescent reporter expression mainly in RIC and AIZ neurons. Surprisingly, the expression in AIZ was stochastic, whereas the expression in RIC was observed in all animals. The decision to express or not was affected apparently by the potential of gene expression that represent, for example, the copy number of the transgenes. A greater potential of gene expression results in a greater probability of expression in AIZ neurons. This expression system enabled the detection of a moderate increase, by approximately twofold, of fluorescent reporter expression by converting it to all-or-none expression states in AIZ neurons. We describe here a successful screen for mutations that generally enhance the expression of transgenes in somatic cells of *C. elegans* by taking advantage of this expression system.

## MATERIALS AND METHODS

### Strains

*C. elegans* strains were cultured and maintained using standard procedure (Brenner 1974) except that NA22 *E. coli* strain was used as food source. The following strains were used: wild-type Bristol strain (N2), wild-type Hawaiian strain (CB4856), *ttTi5605 II*; *unc-119(ed3) III*, *unc-119(ed3) III*; *cxTi10882 IV*, *pqe-1(pe334) III*, *pqe-1(pe335) III*, *pqe-1(pe336) III*, *pqe-1(ok1983) III*, *pels303[lin-11pAΔ::venus, tdc-1p::mRFP, rol-6(d)] X*, *pels304[lin-11pAΔ::venus, tdc-1p::mRFP, rol-6(d)] I*, *pels1334[osm-10p::venus::unc-2(3' UTR), unc-122p::mCherry]*, *pels1336[osm-10p::venus::unc-54(3' UTR), unc-122p::mCherry]*, *pels1338[sra-6p::venus::unc-2(3' UTR), unc-122p::mCherry]*, *pels1339[sra-6p::venus::unc-54(3' UTR), unc-122p::mCherry]*, *pels1090[sra-6p::ChR2::venus, unc-122p::mCherry]*, *mIs13[myo-2::GFP, pes-10::GFP, F22B7.9::GFP] I*, *pels1323[lin-11pA::venus] II*, and *pels1326[lin-11pA::venus] IV*. *pqe-1(pe334)*, *pqe-1(pe335)*, and *pqe-1(pe336)* mutants were obtained in a forward genetic screen for mutants that increase the AIZ expression of *pels304*, *pels303*, *pels304*, *pels1334*, *pels1336*, *pels1338*, *pels1339*, and *pels1090* were produced by the insertion of extra-chromosomal arrays into chromosomes by  $\gamma$ -ray irradiation or MMS (*i.e.*, methyl methanesulfonate) treatment. Other strains were kindly provided from Caenorhabditis Genetics Center (University of Minnesota, St. Paul, MN). *pqe-1(pe334)*, *pels303*, *pels304*, *pels1334*, *pels1336*, *pels1338*, *pels1339*, and *pels1090* were backcrossed to N2 (wild-type) more than three times before characterization.

### Plasmid construction

Plasmids were generated by the GATEWAY system (Invitrogen) as described (Matsuki *et al.* 2006). The entry vectors that contain *lin-11p* (1338 bp) (Hobert *et al.* 1998), *sra-6p* (4005 bp) (Troemel *et al.* 1995), *H20p* (2479 bp), *pqe-1p1* (2299 bp), and *pqe-1p2* (2082 bp) were created by BP reactions (site-directed recombination) between a polymerase chain reaction (PCR)-amplified promoters and the pDONR201 plasmid. *lin-11pA*, *lin-11pB*, and *lin-11pC* were produced by cloning PCR-amplified fragments of 660 bp, 367 bp, and 361 bp, respectively, into *DraI*-digested *pENTR-sra6p*. *lin-11pAΔ* was produced by removing the 80 bp region of *lin-11pA*. The deletion was introduced by PCR amplification of the rest of the plasmid by primers 5'-TAGCGACTATGAATATCTAA-3' and 5'-CTTGAATGTGTCC CCATCAT-3', and then the product was circularized by ligating the ends.

The destination vectors that contain open reading frames (ORFs) of each gene were generated by cloning the cDNA fragment of the gene of interest into the pDEST vector. ORFs for *venus*, *mRFP*, and *mCherry* were amplified from pPD-venus [carrying a modified version of Venus (Nagai *et al.* 2002), which was a gift from T. Ishihara, Kyushu University, Fukuoka, Japan], pRSETb (a gift from R. Tsien, Stanford University School of Medicine), and pWD176 (carrying a optimized mCherry produced by K. Oegema, which was a gift from E. Jorgensen, and subcloned into pDEST by H. Ohno), respectively. The cDNAs of *pqe-1* isoforms were amplified from reverse transcripts of total RNA. The pDEST plasmid of *venus*-fused *pqe-1C* was produced by inserting termination codon-deleted *pqe-1C* ORF in front of the *venus* gene of pDEST-venus. For the pDEST constructs with *unc-2* 3'UTR, a pDEST vector with 853 bp of *unc-2* 3'UTR, which was PCR-amplified by two primers, 5'-CAACCGTTTAAACAAAGCCTCTC-3' and 5'-TTGCGTTCCTCCAATTCT-3', was used. The expression constructs were produced by LR reaction between the entry plasmids and the destination plasmids. Details of the use of the GATEWAY system are available at our web site: [http://park.itc.u-tokyo.ac.jp/mgrl/IINO\\_lab/Gateway/Gateway\\_overview1.html](http://park.itc.u-tokyo.ac.jp/mgrl/IINO_lab/Gateway/Gateway_overview1.html).

### Germline transformation

Transgenic strains were produced by injecting DNA into the gonad of adult animals as described (Mello *et al.* 1991). Expression constructs for *lin-11p* variants were injected at 30 ng/ $\mu$ L along with *unc-122p::mCherry* (10 ng/ $\mu$ L) as a transformation marker and pPD49.26 (60 ng/ $\mu$ L) as carrier DNA except that *lin-11pAΔ::venus* was injected at 30 ng/ $\mu$ L along with *tdc-1p::mRFP* (30 ng/ $\mu$ L) for marking RIC neurons and pRF4[*rol-6(d)*] (40 ng/ $\mu$ L) for inducing roller phenotype. For examination of the promoter activity of *pqe-1*, *pqe-1p1::venus* and *pqe-1p2::mCherry* were injected at 30 ng/ $\mu$ L each along with pPD49.26 (40 ng/ $\mu$ L). *PQE-1C::Venus*-expressing line was produced by injecting *H20p::pqe-1C::venus* (60 ng/ $\mu$ L) along with *H20p::fib-1::mCherry* (5 ng/ $\mu$ L), for marking the nucleoli, and pPD49.26 (35 ng/ $\mu$ L). For rescue experiments of *pqe-1(pe334)*, a PCR-amplified 15-kb fragment (1 ng/ $\mu$ L) or promoter-fused *pqe-1* cDNAs (10 ng/ $\mu$ L) was injected along with *myo-3p::mRFP* (10 ng/ $\mu$ L) as transformation marker and pPD49.26 (80 ng/ $\mu$ L). Germline transformation using the MosSci method was performed as described (Frøkjær-Jensen *et al.* 2008).

### Assay of AIZ phenotypes

Unless otherwise noted, adult animals were prepared by placing six parent adults on each 6-cm Petri dish, which was seeded with NA22 *E. coli*, and letting the offspring grow at 20° for four days. The phenotypes of adults were assayed by counting randomly selected animals

under a fluorescence stereomicroscope (Leica M165 FC). For rescue lines, the phenotypes were checked after we randomly selected animals that possessed the transformation marker. L1 larvae were prepared by incubating the eggs in M9 buffer for about 6 hours after lysing the 4-day-old adults with bleach mix (1N NaOH 0.5 mL, 0.2 mL household bleach [5% solution of NaClO]). Hatched L1 larvae were mounted on an agar pad, and the phenotypes were tested under a epifluorescence microscope (Axioplan2) with 20× or 40× objective.

### Forward genetic screen

Mutagenesis was performed as described (Brenner 1974). A total of 18,000 F1 progeny of mutagenized *pels304* animals were divided into 12 groups; 3000 F2 embryos were collected from each group and raised to adults. The phenotypes of individual F2 adults were observed under a fluorescence stereomicroscope (Leica M165 FC) and AIZ-2ON animals were independently isolated from each group. The F3 progeny of each isolated animal were tested for whether the population shows high rate of AIZ-2ON phenotype. The lines with the most obvious phenotype were selected from each group. Mapping of the responsible mutations in the obtained strains was performed using the SNPs between the N2 Bristol and CB4856 Hawaiian wild-type (Wicks *et al.* 2001). After identifying the chromosomes in which the mutations resided, mapping was focused on *pe334*, *pe335*, and *pe336*, which showed linkage to chromosome III.

### Quantification of fluorescence intensity

The total intensity of Venus in a cell was quantified in L1 larva as previously described (Yamada *et al.* 2010). Nonconfocal fluorescence images of target cells were taken by 100× objective for RIC, AIZ, and ASH neurons and 40× objective for posterior bulb of the pharynx with Zeiss Axioplan2 epifluorescence microscope equipped with a Hamamatsu ORCA-ER camera. The length of exposure was 10 ms for *pels1334*, *pels1336*, and *pels304[tdc-1p::mRFP]*; 100 ms for *pels303*, *pels304[lin-11pΔΔ::venus]*, *pels1090*, *pels1339*, and *mIs13*; 200 ms for low copy–inserted transgenes, *pels1323* and *pels1326*; and 500 ms for *pels1338*. Photos were processed with Metamorph software (Molecular Devices), and the total intensity for the neuronal cell body of each animal was calculated by the equation below.

$$\text{Total intensity} = [(\text{average intensity of the ROI}) - (\text{average intensity of background})] \times (\text{pixels of the ROI})$$

Total intensity was normalized by the average of the control conditions.

### Quantitative real-time PCR

The total RNA of the worms was extracted from L1 larvae. The L1 larvae were obtained by incubating eggs for 12 hr in M9 buffer after collecting eggs from bleached 4-day-old adult animals. Proteins were removed and nucleic acid was recovered with Trizol (Invitrogen) followed by isopropanol precipitation. The nucleic acid extracts were processed with DNase I (QIAGEN) and RNeasy MinElute cleanup kit (QIAGEN) to remove the contaminating DNA and reverse-transcribed by PrimeScript RT reagent Kit (Takara). Quantification of the reverse transcripts was performed by using SYBR RT-PCR kit Perfect real time (Takara) and ABI PRISM7000 (Applied Biosystems) according to the manufactures' protocol. A total of 200 ng of total RNA was reverse-transcribed to cDNA, and an equal amount of cDNA was subjected to a gene-specific PCR in a total volume of 25 μL. Serial dilutions of cDNA prepared from total RNA of wild-

type worms were used to generate a standard curve. The relative quantity of venus transcripts was calculated using the amount of *lmn-1* transcript as a reference, and the results of duplicated experiments for a same sample were averaged.

The primers used for the amplification of each gene were as follows: *lmn1*-F: 5'-CGTTCACCACCCAGAA-3', *lmn1*-R: 5'-CAAGACGAGCTGATGGGTTATCT-3' for *lmn-1*; *venusRT*-F: 5'-TGGAGAGGGTGAAGGTGATG-3', *venusRT*-R: 5'-GACAAGTGTGGCCATGGAA-3' for *venus*; *lin11*-F: 5'-CGCAACACCCAAACCAACTC-3', *lin11*-R: 5'-GAAACCACACCTGAATGACTCTC-3' for *lin-11*; *osm10*-F: 5'-CAACCACAGAATGGCAATCG-3', *osm10*-R: 5'-CGAGCCAAGTCTCTGCAATG-3' for *osm-10*; *myo2*-F: 5'-TGAAGTTC AAGCAACGTCCA-3', *myo2*-R: 5'-GTGGACGAGTCAAAGCCTT C-3' for *myo-2*; *cdc42*-F: 5'-CTGCTGGACAGGAAGATTACG-3', *cdc42*-R: 5'-CTCGGACATTCTCGAATGAAG-3' for *cdc-42*; and *pmp3*-F: 5'-GTTCCCGTGTTCATCACTCAT-3', *pmp3*-R: 5'-ACACCGTCGAGAAGCTGTAGA-3' for *pmp-3*. The primers for *cdc-42* and *pmp-3* were adopted from the previous report (Hoogewijs *et al.* 2008). All primers were designed to include an intron in the PCR product amplified from the genomic DNA for each gene to distinguish them from the product amplified from the cDNA.

The copy numbers of transgenes were quantified by almost the same method. 10 ng of purified genomes were extracted from adult animals and used as templates. The primers used for the amplification of *venus* were: *venus-copy-N-count*-F: 5'-CCAGACAACCATTACC TGTCC-3' and *venus-copy-N-count*-R: 5'-CATCCATGCCAAGTGTAAATCC-3'. The relative copy number was calculated by normalizing by the PCR products that were amplified from a specific region of the genome by using two primers: *copy-N-control*-F: 5'-GTCCGCTTG AAGTTCTCTC-3' and *copy-N-control*-R: 5'-CTCCATTGAATCG TGACCAA-3'.

### Statistical analyses

Error bars in the figures indicate SEM. The statistical analyses for AIZ phenotypes were performed with  $\chi^2$  tests. In cases in which multiple times of tests were required, the analyses were corrected by the use of Bonferroni's method. For the statistical analyses for quantified fluorescence intensity and transcript numbers, Student's *t*-test or Dunnett's test for multiple comparisons was performed.

## RESULTS

### Truncated promoter of *lin-11p*, *lin-11pΔΔ*, drives reporter expression in RIC and AIZ

The third intron of the *lin-11* gene, which encodes a LIM homeodomain transcription factor (Freyd *et al.* 1990), is one of the promoter/enhancers that drive gene expression in AIZ neurons and is denoted here as *lin-11p*. Consistent with the previous report, *lin-11p::venus*, in which a fluorescent reporter *venus* is fused to *lin-11p*, drove strong expression in ADL, ADF, AVJ, RIC and weak expression in RIF and AVG (Hobert *et al.* 1998) (Figure 1, A–C, and supporting information, Figure S1A and Figure S1B). However, only a small fraction of transgenic animals demonstrated reporter expression in AIZ. To finely characterize this unstable reporter expression in AIZ, we first tried to develop truncated promoter/enhancers to specify the expression in AIZ. The third intron of *lin-11* had no obvious TATA box for transcription initiation, making it difficult to design truncated promoter/enhancers. Therefore, subregions of *lin-11p*, segments A, B, and C, were subcloned and connected to the TATA box of the promoter of *sra-6* (Troemel *et al.* 1995) (Figure 1A). The segment C of the *lin-11p* drove expression in AVJ (Figure S1I, Figure S1J, Figure S1K, and

Figure S1L), whereas the segment A drove expression in ADL, ADF, RIC, and AIZ (Figure S1E, Figure S1F, Figure S1G, and Figure S1H). In contrast, segment B drove no expression, suggesting that this segment includes no obvious enhancer function. We further truncated segment A and found that the truncated promoter, *lin-11pAΔ*, was sufficient for the expression in RIC and AIZ, whereas the expression in ADL and ADF was weakened in this promoter (Figure 1, D and E, Figure S1C and Figure S1D).

### *lin-11pAΔ* drives stochastic reporter expression in AIZ

In *C. elegans*, transgenes introduced by microinjection are usually held as an extra-chromosomal array, which is randomly lost during cell divisions (Stinchcomb *et al.* 1985). To exclude the effect of mosaicism, we integrated the extra-chromosomal transgenes of *lin-11pAΔ::venus* into the chromosomes by  $\gamma$ -ray irradiation. This treatment yielded two integrants, *peIs303* and *peIs304*, in which the transgene *lin-11pAΔ::venus* was inserted into chromosome X and I, respectively. Both *peIs303* and *peIs304* animals showed stochastic expression in AIZ. *C. elegans* has two bilaterally symmetric AIZ neurons, AIZL and AIZR, and we found all four types of combinations of expression patterns, 2ON, rightOFF/leftON, rightON/leftOFF, and 2OFF in both integrants (Figure 2A; ON and OFF indicate that the expression is observed and not observed, respectively, in each cell). Because the numbers of rightOFF/leftON animals and rightON/leftOFF animals were almost the same, we did not distinguish them further and combined them as 1ON/1OFF. The distribution of AIZ phenotypes was different in the two integrant lines with a greater rate of expression in AIZ in *peIs303* animals. On the other hand, there was no significant difference between L1 larvae, the first larval stage just after hatching, and adult animals in each strain (Figure 2B). When individual *peIs304* animals were isolated at the L1 stage, sorted by their AIZ expression phenotypes and cultured further, they showed the same phenotypes 3 days later when they grew up to adults (Figure 2C). These results indicate that the phenotypes of AIZ expression are decided at the early stage of development and maintained throughout the individuals' life. Furthermore, the progeny of isolated *peIs304* individuals showed the distribution of phenotypes identical to their mother's generation irrespective of their mother's phenotype (Figure 2D and Figure S2). Therefore, the AIZ expression phenotypes are not inherited but decided by chance during embryogenesis.

### Probability of *lin-11pAΔ::venus* expression in AIZ is correlated with the strength of its expression in RIC

Through a series of observations of the reporter expression from *peIs303* and *peIs304*, we noticed that *peIs303* shows stronger reporter expression than *peIs304*. To clarify this, we compared the reporter expression in RIC because all animals harboring *lin-11pAΔ::venus* show reporter expression in RIC. The quantified fluorescence intensity in RIC of *peIs303* was more than twice that of *peIs304* (Figure 2E). Because the probability of reporter expression in AIZ was greater in *peIs303* than in *peIs304* (Figure 2B), these results suggest that the greater rate of "ON" expression of *lin-11pAΔ::venus* in AIZ in *peIs303* animals may be caused by stronger expression induction potential of the transgene. To demonstrate the causal relationship between the potential of expression induction and probability of AIZ expression, we tested the AIZ phenotypes of heterozygotes of *lin-11pAΔ::venus* integrants. We crossed *peIs303* or *peIs304* homozygous animals to animals that carry a dominant genetic marker with wild-type background. As expected, resulting heterozygous animals, *peIs303/+* and *peIs304/+*, showed lower rates of AIZ-ON phenotype than homozy-

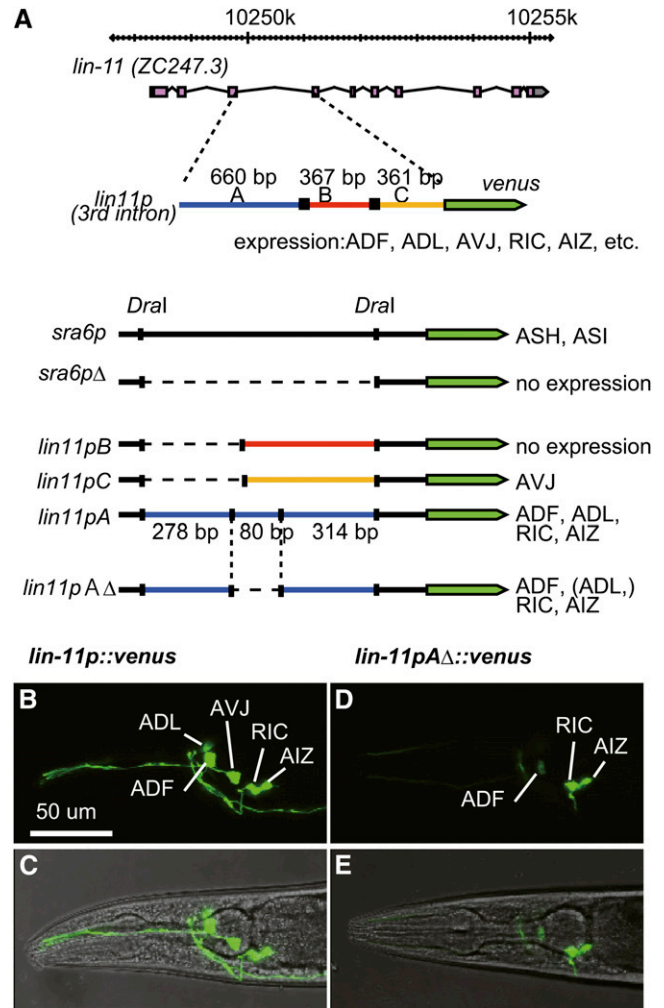


**Figure 1** Production of a promoter to restrict the reporter expression in RIC and AIZ. (A) Illustration of the construction of composite promoters. The 4-kb promoter of *sra-6* was digested by a restriction enzyme, *Dral*, and ligated to exclude a 3.6-kb region. The resulting promoter *sra-6pΔ* did not induce expression of the fused reporter gene. The segments of *lin-11p*, A, B, and C, were introduced to the *sra-6pΔ* to produce *lin-11pA*, *lin-11pB*, and *lin-11pC*, respectively. *lin-11pA* was further truncated to produce *lin-11pAΔ*. (B–E) Expression pattern of *lin-11p::venus* and *lin-11pAΔ::venus*. The third intron of *lin-11* (B and C) or the synthetic promoter *lin11pAΔ* (D and E) was fused to *venus* cDNA and introduced to wild-type animals to examine the promoter activity. The fluorescence image of the head and the image merged with bright field image of an adult animal are shown in (B and D) and (C and E), respectively.

gous animals, *peIs303/peIs303* and *peIs304/peIs304*, supporting the idea that the stronger expression induction potential of *lin-11pAΔ::venus* leads to a greater rate of AIZ-ON phenotype (Figure 2F).

It was possible that the reporter expression in AIZ was generally weaker than that in RIC, and therefore the reporter expression in some animals was below threshold of detection only in AIZ but not in RIC. However, this is not the case because the average fluorescence intensity of the reporter expression in AIZ among the animals in which we could observe the expression in AIZ was almost the same as the average intensity in RIC (Figure 2G). These results suggest that AIZ has two discrete expression states corresponding to ON and OFF and somehow the expression induction potential determines the

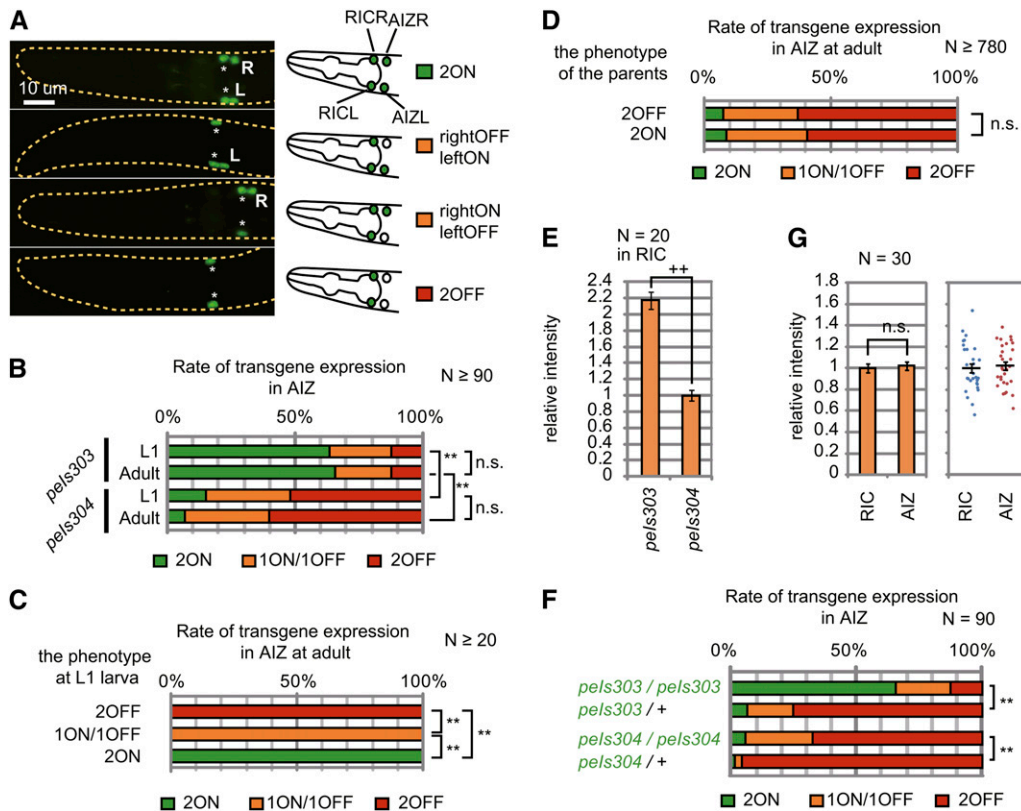


**Figure 2** Genome-integrated *lin-11pAΔ::venus* drives stochastic expression in AIZ neurons. (A) The individual expression pattern of *pels304[lin-11pAΔ::venus]* in an isogenic population of L1 larvae. All the animals in a population showed reporter expression in RIC neurons, whereas the expression in AIZ neurons were stochastic. The illustrations at the right side summarize the phenotype in the left picture. \*, L, and R indicate RIC neurons, AIZL, and AIZR, respectively. (B) AIZ phenotype of *pels303* and *pels304* animals at L1 larval and adult stages. The L1 animals were observed within 6 hr from hatch and the adults were tested on the fourth day after putting the parents on the plates ( $n \geq 90$ ). (C) AIZ phenotype of adult *pels304* animals that were isolated at L1 larva and classified according to their AIZ phenotypes ( $n \geq 20$ ). (D) AIZ phenotypes of the offspring of the *pels304* animals with indicated phenotypes. The AIZ phenotypes of the offspring were tested at adult ( $n \geq 780$ ). (E) Normalized fluorescence

intensity from *pels303* and *pels304* in RIC neurons of L1 larvae ( $n = 20$ , error bars represent SEM). (F) AIZ phenotypes of heterozygous integrant animals at adult. A dominant genetic marker, *mIs13[myo-2p::gfp]*, was used to verify successful cross. (G) Normalized fluorescence intensity from *pels304* in RIC and AIZ neurons of L1 larva. The fluorescence intensity was quantified in the animals that showed reporter expression in AIZ neurons. Scatter plot in the right graph indicates the data of individual neurons ( $n = 30$ , Error bars represent SEM). \*\*Significant differences at  $P < 0.001$  by  $\chi^2$  test; ++significant difference at  $P < 0.001$  by Student's t-test. n.s. indicates that they are not significantly different at  $P < 0.01$  by  $\chi^2$  test or Student's t-test.  $\chi^2$  tests in (B, C, and F) were corrected by Bonferroni's method)

probability of the ON state through a thresholding effect in AIZ (see Discussion). In contrast, the expression in RIC does not seem to show such transformation.

The difference of the expression level between *pels303* and *pels304* could be attributable to the difference in copy number of transgenes integrated into each genomic locus, the structures of the multicopy transgenes, or location of genomic insertion. To determine the copy number of transgenes, we compared the copy number of *pels303* and *pels304* to low copy genomic insertions produced by MosSCI. MosSCI, *Mos1*-mediated Single Copy transgene Insertion, is a technique to insert transgenes into *Mos1* transposon-inserted genomic loci through repair of *Mos1* excision events, resulting in low copy insertion of the transgenes (Frøkjær-Jensen *et al.* 2008). By using this technique, we inserted *lin-11pA::venus* into two loci, *tTi5605 II* and *cxTi10882 IV*, in the genome and obtained two alleles, *pels1323* and *pels1326*, respectively. We extracted the genome from transgenic animals and compared the copy number of the *venus* gene by real-time PCR. Because MosSCI generally produces single copy insertion with less than 10% of duplicated insertion and the relative copy number of *venus* in *pels1326* was exactly twice that of *pels1323*, we could speculate that *pels1323* was a single-copy insertion and *pels1326* was a duplicated-copy insertion (Figure S3). Compared with these low copy transgenes, the *venus* copy numbers in *pels303* and *pels304* were estimated to be 34(+/-8) and 35(+/-13), respectively. The estimated copy numbers of transgenes in *pels303* and *pels304* were not signif-

icantly different, and therefore the difference in AIZ phenotype may arise from other factors, such as the difference in the structure of the transgenes or different locations in the genome.

### Mutations in the *pqe-1* gene enhance the expression of *lin-11pAΔ::venus*

To screen for mutations that enhance the expression of transgenes in *C. elegans*, we took advantage of the expression system of *pels304*, in which a moderate increase in expression induction potential is converted to a drastic change from AIZ-OFF to AIZ-ON through the thresholding effect observed in AIZ. We mutagenized *pels304* animals and screened for mutations that cause a greater rate of reporter expression in AIZ. Such a phenotype could be caused by an upward shift of the distribution of expression inducing potential. Of 12 independent mutations isolated by the screen, *pe334*, *pe335*, and *pe336*, were mapped to the center of chromosome III, whereas the others were mapped to the center of chromosome I. Because the mutations that were mapped to chromosome I showed strong linkage to the inserted transgene, *pels304*, it was likely that these mutations occurred in the *pels304* allele itself.

Therefore, we focused on the mutations on chromosome III for further analyses. Mutants of all three alleles showed almost 100% of AIZ-2ON phenotype (Figure 3A). Among those mutations, *pe334* was mapped to a region of 26 kb between two SNPs, *haw43145* and *haw43156* (Figure 3B). There were only four genes in this interval,

and among them we found a nonsense mutation in the *pqe-1* gene. We concluded *pqe-1* was responsible for the high frequency of AIZ-2ON phenotype for the following three reasons. First, the *pe335* and *pe336* mutants also possessed nonsense mutations in the *pqe-1* gene (Figure 3B). Second, a 1330-bp deletion in the *pqe-1* gene, *ok1983*, also caused a high frequency of AIZ-2ON phenotype when combined with *pels304* (Figure 3, A and B). Finally, the introduction of a PCR fragment spanning the *pqe-1* gene and the adjacent gene *F52C9.7*, within which our mutants do not have any mutations, rescued the AIZ-2ON phenotype of the *pe334* mutant (Figure 3, B and C). For the aforementioned reasons, we re-define the nonsense mutation in *pqe-1* gene in each mutant as *pqe-1(pe334)*, *pqe-1(pe335)*, and *pqe-1(pe336)* (Figure 3B).

Along with the rescue of the AIZ phenotype, introduction of genomic *pqe-1* fragments into the *pqe-1(pe334)* mutant also caused silencing of reporter in RIC, which was consistently expressed in the original *pels304*; *pqe-1(+)* animals (Figure 3C, Figure S4A, Figure S4B, Figure S4C, Figure S4D, Figure S4E, Figure S4F, Figure S4G, and Figure S4H). The repression of the reporter in RIC may be caused by overexpression of the *pqe-1* gene in the rescue constructs because the extra-chromosomal array also repressed the expression in RIC neurons, as well as AIZ neurons, when transferred into the *pqe-1(+)* background (Figure S4I). These results suggest that, when overexpressed, *pqe-1* acts not only in AIZ but also in RIC and probably in other neurons to suppress the transgene expression regardless of whether they have threshold for expression. To further characterize the effect of *pqe-1* on the AIZ phenotypes, we examined the effect of halved copy number of *lin-11pAΔ::venus* in *pqe-1(pe334)* mutant background. As described previously, the heterozygotes of *lin-11pAΔ::venus*, *pels303/+* and *pels304/+*, show decreased expression in

AIZ (Figure 2E). In the *pqe-1(pe334)* mutant background, the rate of reporter expressions in AIZ from both *pels303/+* and *pels304/+* were increased again, indicating that the mutation in *pqe-1* reversed the effect of decreased transgene copy number (Figure 3D).

*pqe-1* is a nematode-specific gene. Loss of function of this gene by itself shows no obvious phenotype but was reported to enhance the toxicity of overexpression of poly-glutamine (polyQ) (Faber *et al.* 1999, 2002). In these studies, the neurotoxic effect of mutant huntingtin, which causes neurodegenerative Huntington disease in humans, was examined in *C. elegans*. The polyQ region of mutant huntingtin, Htn-Q150, was ectopically expressed in ASH sensory neurons and mutations in *pqe-1* was identified through forward genetic screen as mutations that enhance the neural degeneration by Htn-Q150. *pqe-1* has at least three isoforms, PQE-1B with exonuclease domain, PQE-1C with Q/P rich region and a repeat of nuclear localization signals, and PQE-1A with all these domains [Figure 3B and Figure S5A; note that the naming of the variants are based on the previous report (Faber *et al.* 2002) and different from the isoform names in WormBase (<http://www.wormbase.org>)]. PQE-1C was sufficient for the polyQ toxicity enhancing phenotype (Faber *et al.* 2002). To examine which isoforms are important for the high rate of AIZ-2ON phenotype, we conducted rescue experiments by expressing each isoform pan-neuronally in *pels304*; *pqe-1(pe334)* mutants. As a result, we found that the expression of PQE-1A or PQE-1C isoform could rescue the AIZ-ON defect efficiently, as in the case for polyQ toxicity enhancing phenotype. In these rescue experiments, we observed reduction of reporter repression also in RIC, again probably by the effect of overexpression (Figure 3C). The rescue of the mutant phenotype by PQE-1A and PQE-1C isoforms was the same as the previous study, suggesting that these two phenomena may have common causes.

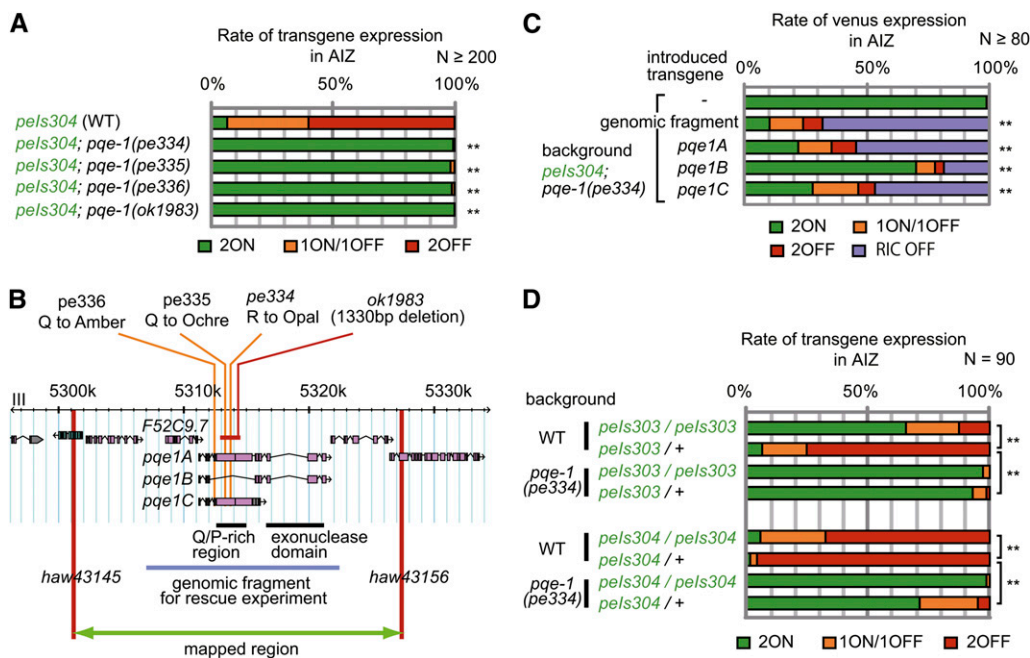


**Figure 3** Mutations in the *pqe-1* gene enhance the reporter expression in AIZ from *pels304*. (A) AIZ phenotypes of mutants, *pe334*, *pe335*, and *pe336*, isolated through mutant screen and an independently isolated deletion mutant of *pqe-1*, *ok1983*, at adult ( $n \geq 200$ ). (B) Locations of identified mutations. *pe334*, *pe335*, and *pe336* were identified as Q to Opal, Q to Ochre, and Q to Amber, respectively. The mapped region and the genomic fragments used for rescue experiments in (C) are indicated. The *pqe-1* gene has three main isoforms, which include either or both of the Q/P rich region and the exonuclease domain. (C) Rescue experiments for *pqe-1(pe334)* mutants. The cDNA of each isoform was expressed by a pan-neuronal

promoter, *H20p*. The transgenes were introduced to mutants as extrachromosomal array by using *myo-3p::mRFP* as a transformation marker. Only the adult animals that carry the extrachromosomal array were used for the analysis. In this graph, the animals that lacked the reporter expression in both RIC and AIZ in either side were counted as RIC OFF. In addition, if a single cell showed expression in either side, that cell was assumed to be RIC ( $n \geq 80$ ). (D) AIZ phenotypes of heterozygous integrant animals in *pqe-1(pe334)* mutant background at adult. *mIs13[myo-2p::gfp]*, was used to verify successful cross ( $n = 90$ ). \*\*Significant differences at  $P < 0.001$  by  $\chi^2$  test with Bonferroni's correction.)

## **pqe-1 is expressed in various tissues and shows dot-like localization in the nuclei**

*pqe-1* is predicted to form an operon with several other nearby genes (C. elegans Sequencing Consortium 1998). To examine the expression pattern of *pqe-1*, we tested two regions, *pqe-1p1*, which is located at upstream of the whole operon, and *pqe-1p2*, which is immediately upstream of *pqe-1*, for promoter activity (Figure 4A). We cloned a 2-kb region of each promoter and tested their expression induction by fusing to *venus* reporter. *pqe-1p1* drove expression in excretory canal, vulval cells, and neurons at the head and the tail, whereas *pqe-1p2* drove expression in intestine and neurons (Figure 4, B–I). The expressing cells were almost different between these two promoters with a small overlap (Figure 4, E and I). We confirmed that the *pqe-1p1* drives reporter expression in sensory neurons including ASH, in which the polyQ toxicity enhancing phenotype of *pqe-1* mutants was previously observed, whereas *pqe-1p2* drives reporter expression in several other neurons, including RIC and AIZ (Figure 4, J and K). Previously, it was reported that PQE-1C protein shows a dot-like localization in the nucleus and functions cell-autonomously (Faber *et al.* 2002). Because we confirmed *pqe-1* promoters drive reporter expression in AIZ, the effect of *pqe-1* on AIZ phenotype may be also cell-autonomous. The most remarkable structure in the nuclei is nucleoli. To test whether PQE-1C localizes to the nucleoli, we expressed PQE-1C::Venus along with the nucleolus marker FIB-1::mCherry (Goldsmith *et al.* 2010; Lee *et al.* 2010) (Figure 4L–P). The intranuclear localization of PQE-1C::Venus (Figure 4N) was different from that of FIB-1::mCherry (Figure 4O), indicating that PQE-1 does not localize to the nucleoli. We speculate that the dots represent the aggregation of PQE-1C proteins because PQE-1C includes high content of glutamine, 112 of 572 amino acids in the Q/P rich region (Figure S5B), and polyQ proteins are known to have trends of aggregation (Williams and Paulson 2008).

## **pqe-1 affects the expression of various transgenes**

The suppression of *pels303* and *pels304* by *pqe-1* overexpression in RIC suggested that *pqe-1* diminishes the potential of expression induction in both RIC and AIZ (Figure 3C and Figure S4I). To confirm this, we quantified the intensity of the reporter fluorescence in RIC in the *pqe-1* mutant background. As expected, we could detect a more than twofold increase in transgene expression in RIC of *pqe-1* mutants (Figure 5A). The polyQ toxicity phenotype in the previous report was observed in ASH by expressing a polyQ region of huntingtin, Htn-Q150, by the promoter of *osm-10* or *sra-6* (Faber *et al.* 2002). To examine whether *pqe-1* mutation also affects the reporter expression from these promoters, we produced transgenic strains with chromosomally integrated *osm-10p::venus* and *sra-6p::venus*, *pels1336* and *pels1339*, respectively. Both of the transgenes showed stronger expression in ASH in the *pqe-1(pe334)* background (Figure 5, B and C). In this study and probably also in the previous report, the *unc-54* 3'UTR was used as the 3'UTR in the transgenes. To exclude the possibility that *pqe-1* regulates the function of *unc-54* 3'UTR, we produced chromosomally integrated transgenic strains with another 3'UTR, *unc-2* 3'UTR. The transgenes with the 3'UTR of *unc-2*, *pels1334* and *pels1338*, also showed increased expression in the *pqe-1(pe334)* background (Figure 5, D and E). We further examined the expression of a chromosomally integrated transgene, *mIs13[myo-2p::gfp]*, which drives expression of another fluorescent reporter gene, *gfp*, in a non-neuronal tissue, namely the muscles in the posterior bulb of pharynx. The reporter expression by *myo-2p::gfp* also increased in the *pqe-1(pe334)* mutant background (Figure 5F, Figure S6A, Figure S6B, and Figure S6C). In addition, we examined the effect of *pqe-1* mutation on

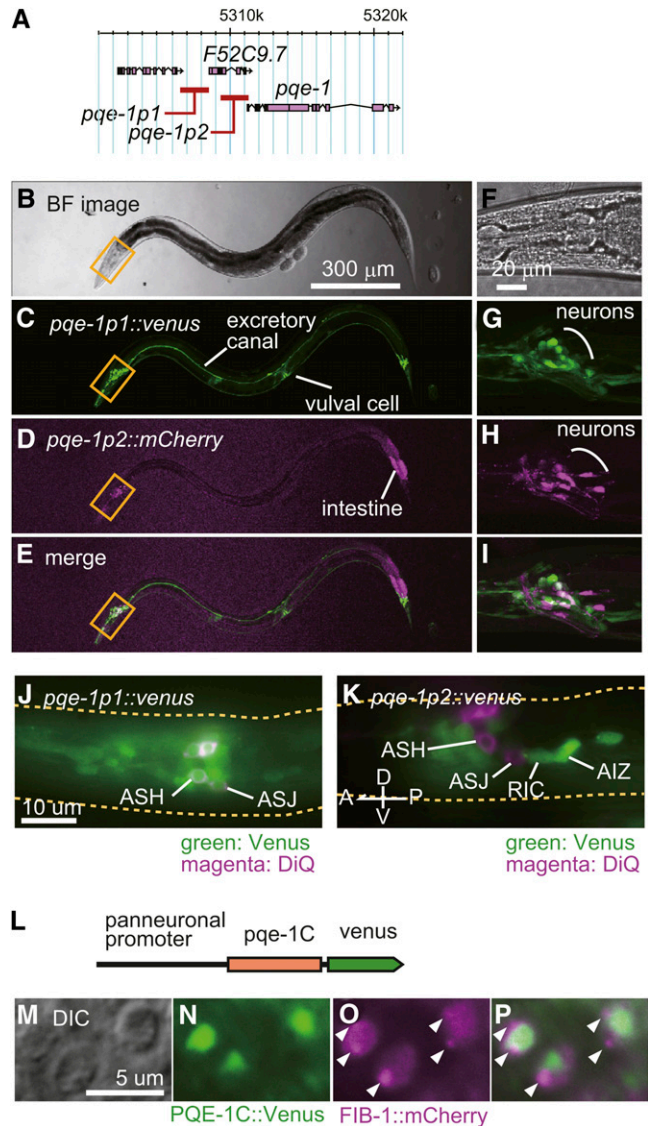


**Figure 4** Expression pattern of *pqe-1* gene and intracellular localization of PQE-1. (A) Promoters used for the expression of fluorescent reporters. *pqe-1p1* and *pqe-1p2* are the 2 kb upstream region of *F52C9.7* and *pqe-1*, respectively. (B–I) Expression patterns of *pqe-1p1::venus* (C and G) and *pqe-1p2::mCherry* (D and H) in an adult animal. (E and I) are merged images of (C and D) and (G and H), respectively. (B and F) are bright-field images of (C–E) and (G–I), respectively. (F–I) are the magnified images of the head region shown by yellow squares in (B–E). (J and K) Expression patterns of *pqe-1p1::venus* (J) and *pqe-1p2::venus* (K) merged with the DiI-stained cells (magenta: ASJ and ASH) in the head. (L–P) Nuclear localization of PQE-1C::Venus. A *venus*-fused *pqe-1C* cDNA is expressed by a pan-neuronal promoter, *H20p* (L). The dot-like localization of PQE-1C::Venus (N) and FIB-1::mCherry in the nucleus (O). (P) is the merged image of (N) and (O). (M) is the DIC image of the region in (N–P). Arrowheads in O and P indicate the nucleolar localization of FIB-1::mCherry.

the expression of mRFP, which was cloned from corals and has low sequence homology with GFP and its variants (Matz *et al.* 1999). The expression of mRFP from *tdc1p::mRFP*, which drives mRFP expression in RIM and RIC neurons and was included in *pels304* to help identification of RIC neurons, was also increased in the *pqe-1(pe334)* mutant background (Figure 5G). Therefore, *pqe-1* affects many types

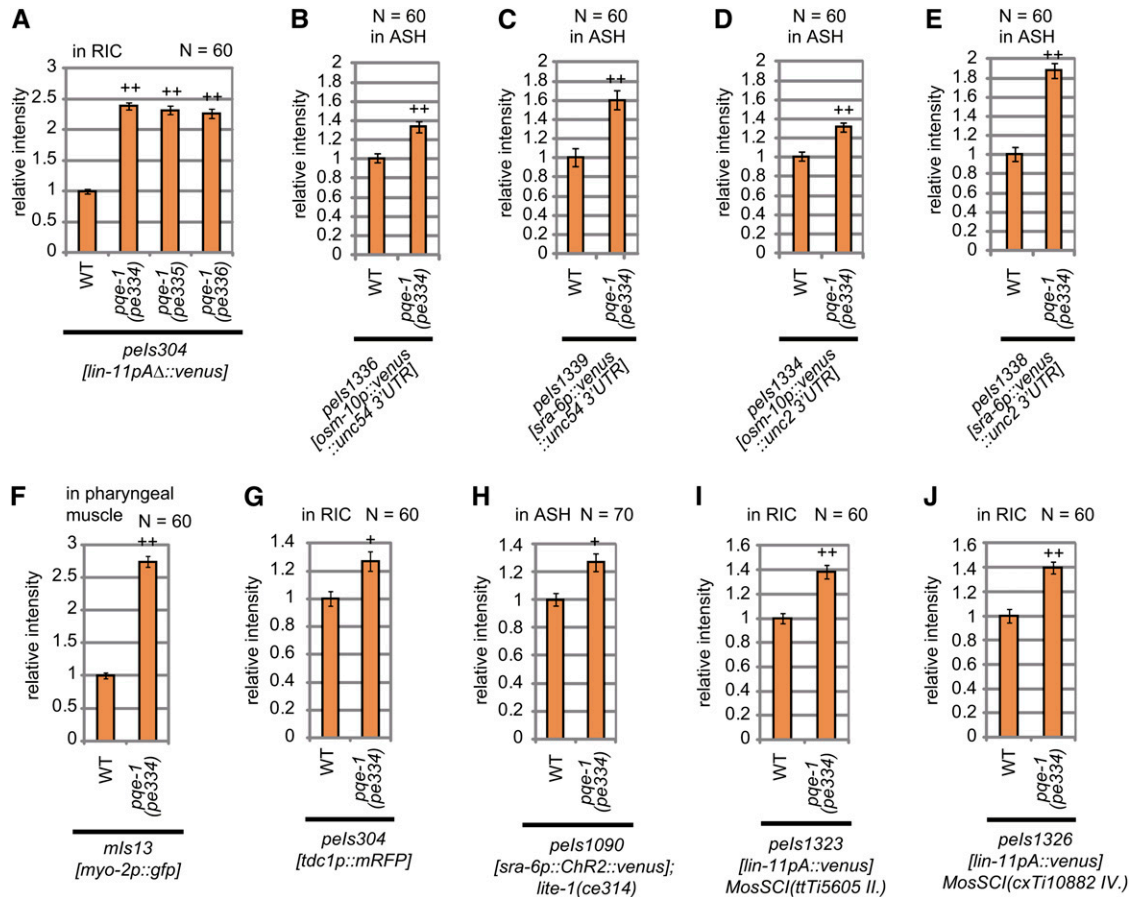


**Figure 5** *pqe-1* mutations enhance the expression of various transgenes. (A) Expression enhancement of *pels304* [*lin-11pAΔ::venus*] in RIC neurons at L1 larva. The average fluorescence intensity in RIC neurons of each mutant is normalized by that of wild-type animals. ( $n = 60$ , Error bars represent the SEM; ++ indicates significant difference at  $P < 0.001$  by Dunnett's test) (B–J) Expression enhancement of transgenes in *pqe-1* (*pe334*) at L1 larva. The cells in which transgenes were expressed and fluorescence intensity was quantified are indicated at the top of the graphs. The normalized fluorescence intensity from transgenes, *pels1336* [*osm-10p::venus::unc-54 3'UTR*], *pels1339* [*sra-6p::venus::unc-54 3'UTR*], *pels1334* [*osm-10p::venus::unc-2 3'UTR*], *pels1338* [*sra-6p::venus::unc-2 3'UTR*], *mIs13* [*myo-2p::gfp*], *pels304* [*tdc-1p::mRFP*], *pels1090* [*sra-6p::Chr2::venus*], *pels1323*, and *pels1326* are shown in (B), (C), (D), (E), (F), (G), (H), (I), and (J), respectively. The *pels304* transgene includes *tdc-1p::mRFP*, which induces *mRFP* expression in RIM and RIC, in addition to *lin-11pAΔ::venus*. In (G), the fluorescence intensity of *mRFP* was quantified. *pels1323* and *pels1326* are low copy insertions of *lin-11pA::venus* into the genome. ( $n \geq 60$ , Error bars represent SEM; + and ++ show significant difference at  $P < 0.01$ , and  $P < 0.001$ , respectively, by Student's *t*-test with Bonferroni's correction.)

of transgenes probably with no specificity of promoters, 3'UTRs, or coded genes. In addition to these integrants, we could observe increase in the expression of Channelrhodopsin-2 fused to Venus (Boyden *et al.* 2005), *pels1090* [*sra-6p::Chr2::venus*], which can be used for optogenetic manipulation of ASH neurons (Figure 5H). These results suggest that *pqe-1* mutations could be used as a tool for increasing the expression of useful transgenes in *C. elegans*.

The chromosomally integrated transgenes used previously were formed by the insertion of multicopy tandem arrays into chromosomes. Multicopy transgenes are known to be regulated by multicopy recognition proteins. In *C. elegans*, several molecules, including a RING finger/B-Box factor TAM-1, a retinoblastoma-like protein LIN-35, and a bromodomain protein LEX-1, were reported to enhance the expression of multicopy transgenes (Hsieh *et al.* 1999; Tseng *et al.* 2007), although little is known about detailed mechanism of antisilencing by these regulators. Because recent progress of MosSCI techniques in *C. elegans* has enabled the production of low copy transgene insertions in the genome (Frøkjær-Jensen *et al.* 2008), we examined whether the *pqe-1* mutation also affects such low copy

transgenes. We tested the effect of the *pqe-1* mutation on *pels1323* and *pels1326*, which were produced by the MosSCI technique (Figure S3). Even the low copy insertions showed stronger expression in the *pqe-1* (*pe334*) mutant background, indicating that the effect of PQE-1 also covers low copy transgenes produced by MosSCI (Figure 5, I and J). Altogether, 10 transgenes were tested and in all of them (10/10) the transgene expression was enhanced by the *pqe-1* mutation (Figure 5).

To examine whether the enhancement of the reporter expression in *pqe-1* mutants was attributable to the increase of transcripts, we performed RT-PCR assay against *venus* transcripts from *pels304* [*lin-11pAΔ::venus*], *pels1336* [*osm-10p::venus::unc-54 3'UTR*], *pels1334* [*osm-10p::venus::unc-2 3'UTR*], *pels1338* [*sra-6p::venus::unc-2 3'UTR*], *mIs13* [*myo-2p::venus*], and *pels1323* [*lin-11pA::venus*] (MosSCI) transgenes. As a result, we could detect a subtle increase of transcripts from *pels1338*, *mIs13*, and *pels1323* in the *pqe-1* (*pe334*) background whereas no increase of transcripts was detected for *pels304*, *pels1336*, and *pels1334*, even though the Venus fluorescence was increased (Figure S7A, Figure S7B, Figure S7C, Figure S7D, Figure S7E, and Figure S7F). PQE-1A and B isoforms possess an exonuclease domain with



homology to REX1, RNA exonuclease homolog 1. Rex1 is known to function in the processing of 3' ends of 5S rRNA and several tRNAs in yeast (Copela *et al.* 2008; Ozanick *et al.* 2009), suggesting that PQE-1 may also function in the regulation of components of the translation machinery. This idea is consistent with our observation that PQE-1 affects transgene expression irrespective of the promoter or the 3'UTR sequences. In this context, the increase of reporter transcripts from the *pels1338*, *mIs13*, and *pels1323* transgenes in *pqe-1* mutants may be a side effect of the increase of general translation. Alternatively, subtle increases in the transcripts, sometimes below threshold of detection, may be the primary cause of the *pqe-1* defect. Notably, no increase in transcription was observed for any of the endogenous genes that we tested, suggesting that transgenes are specifically recognized by PQE-1 (Figure S7G, Figure S7H, Figure S7I, Figure S7J, and Figure S7K).

## DISCUSSION

### The mechanisms of stochastic expression in AIZ

In this study, we observed two discreet states of reporter expression in AIZ neurons, denoted as AIZ-ON and AIZ-OFF. These states are apparently selected in a stochastic manner early in development and remain stable until adulthood. To explain the cause of this stochastic selection, we consider three possible mechanisms. First, this type of bistable behavior is often manifested by regulatory networks having either positive or double-negative feedback loops (Acar *et al.* 2005; Ferrell 2002; Mettetal *et al.* 2006; Ozbudak *et al.* 2004). The caveat is that in our case, the products of the transgenes are fluorescent proteins, which would not be expected to participate in a feedback loop. However, it is still possible that regulatory regions in the transgenes, other than the open reading frame, act in the feedback regulation. For example, if an unidentified miRNA is encoded in the composite promoter, *lin-11pAΔ*, it could form a feedback loop by down-regulating a putative regulator that, in turn, could negatively regulate the expression from the *lin-11pAΔ* promoter (Figure S8A). Second, binary transition of the gene expression unit is also possible. For example, cooperative switching in the chromatin compaction similar to the transition between heterochromatin and euchromatin can easily establish all-or-none expression states (Figure S8B). In this case, the greater potential for transcription probably results in a greater probability of the euchromatin form. Because the homologous chromosomes would be regulated independently, some fraction of cells should show intermediate reporter expression. However, we did not observe such a stepwise distribution of reporter expression (Figure 2G), making this chromatin regulation model less likely. Finally, we propose another model by epigenetic chromatin remodeling which does not accomplish all-or-none expression decision but fixes the rate of transcription at some level. Once the promoter activity is fixed, it can be translated to a quasi-binary output if a threshold effect is imposed. This threshold could be caused by a strong degradation system that degrades mRNA or protein product efficiently, but is limiting in its capacity. As a consequence, mRNA or protein product accumulates only when the rate of synthesis exceeds the degrading capacity, and above this threshold, the accumulation of the product steeply increases until it reaches the maximal capacity of the gene expression system (Figure S8C). In any case, some of the components of the regulatory system that cause binary expression of the fluorescent reporter must be operative in AIZ but absent in RIC. The regulation by *pqe-1* appears to be part of the general mechanism shared by both neuronal types. Although the precise mechanisms of the peculiar characteristic of transgene expression in AIZ are still obscure, AIZ neurons are

involved in multiple behaviors, and therefore the individuality of gene expression may be expressed as behavioral differences.

### The function of PQE-1

In the previous report, *pqe-1* was identified in a screen for mutations that enhance the toxicity of ectopic expression of the polyQ protein (Faber *et al.* 2002). As is the case in patients with Huntington's disease, the expression of Htn-Q150, which is the N terminal part of mutant human huntingtin carrying an expanded polyQ repeat, in the ASH neurons caused neural death in *C. elegans* (Faber *et al.* 1999). On the basis of our study, the polyQ toxicity-enhancing phenotype in *pqe-1* mutants could be caused by the enhancement of expression of Htn-Q150 in ASH neurons. The authors of the previous report observed no change in the fluorescence of the GFP reporter in *pqe-1* mutants. However, a careful quantification of fluorescence intensity would have been required to reveal the effect of *pqe-1* on the enhancement of transgene expression because *pqe-1* mutations increase the transgene expression only by 2.5-fold at most, and the effect of *pqe-1* mutation differs among integrants (Figure 5).

Our study suggested that *pqe-1* regulates the expression of a wide range of transgenes, possibly through controlling the translation machinery or recognizing epigenetic markers on transgenes to suppress transcription. The rescue experiments with PQE-1 isoforms indicated that the Q/P-rich region was more important than the exonuclease domain (Figure 3, B and C). However, this Q/P-rich region is not really conserved even among the nematode species except that the domain includes high content of glutamine and proline, about 20% of glutamine and about 15% of proline (Figure S5B). PQE-1C isoform shows a dot-like localization in the nucleus (Figure 4, L–P) (Faber *et al.* 2002), and therefore Q/P-rich region probably induces aggregation and the aggregation may be important for controlling the function of the long isoform. Hypothesizing that the Q/P-rich region is required for the aggregation of PQE-1 for its function, it would be reasonable that rather than the amino acid sequences but the content of glutamine and proline in Q/P-rich region are conserved among PQE-1 in related species.

### The application of *pqe-1* mutation to enhance the expression of transgenes in *C. elegans*

Because the PQE-1C isoform is strongly localized in the nucleus, it probably acts cell-autonomously as reported previously (Faber *et al.* 2002). We examined two candidate promoter sequences of *pqe-1*, *pqe-1p1*, and *pqe-1p2*, and observed the reporter expression in excretory canal, vulval cells, intestine, and many neurons. Although we did not find expression by these promoters in the pharyngeal muscle in which *mIs13[myo-2p::gfp]* is expressed, the *pqe-1(pe334)* mutation enhanced the transgene expression also in this tissue (Figure 5F and Figure S6). This discrepancy is probably caused by the insufficiency of the *pqe-1* promoter regions that we used to examine the expression pattern of *pqe-1*; *pqe-1* may be actually expressed in many other tissues, and in that case the *pqe-1* mutations may have effects in a broader range of tissues than we have assumed.

The *pqe-1* mutation enhanced expression of transgenes with no specificity to promoters, 3'UTRs, nor coded genes. In addition to this nonspecificity, the *pqe-1* mutation can also affect low copy transgenes produced by MosSCI. Low expression level of transgenes sometimes hampers the use of transgenes in genetic manipulations. Specifically, many recently developed techniques in *C. elegans* such as genetic ablation (Chelur and Chalfie 2007), cell-specific knock-down (Esposito *et al.* 2007), and optogenetic manipulation (Nagel *et al.*

2005; Zhang *et al.* 2007) require high expression level of transgenes. We found no obvious defect in *pqe-1* mutants other than enhancing the expression of transgenes, and therefore they would be a useful tool for maximizing the effect of transgenes. This strategy cannot be readily applied to other model organisms because *pqe-1* is a nematode-specific gene. However, further exploration in other organisms may lead to the discovery of other genes similar to *pqe-1* that also suppress general transgene expression.

## ACKNOWLEDGMENTS

We thank the *Caenorhabditis* Genetic Center, which is funded by National Institutes of Health National Center for Research Resources, for the *C. elegans* strains used in this study. We also thank members of our laboratory for useful advice and discussion. This work was supported by the Grant-in-Aid for Scientific Research (B) and Grant-in-Aid for Scientific Research on Innovative Areas “Systems Molecular Ethology” from the Ministry of Education, Culture, Sports, Science and Technology (MEXT).

## LITERATURE CITED

- Acar, M., A. Becskei, and A. van Oudenaarden, 2005 Enhancement of cellular memory by reducing stochastic transitions. *Nature* 435: 228–232.
- Boyden, E. S., F. Zhang, E. Bamberg, G. Nagel, and K. Deisseroth, 2005 Millisecond-timescale, genetically targeted optical control of neural activity. *Nat. Neurosci.* 8: 1263–1268.
- Brenner, S., 1974 The genetics of *Caenorhabditis elegans*. *Genetics* 77: 71–94.
- C. elegans* Sequencing Consortium, 1998 Genome sequence of the nematode *C. elegans*: a platform for investigating biology. *Science* 282: 2012–2018.
- Chalfie, M., Y. Tu, G. Euskirchen, W. W. Ward, and D. C. Prasher, 1994 Green fluorescent protein as a marker for gene expression. *Science* 263: 802–805.
- Chelur, D. S., and M. Chalfie, 2007 Targeted cell killing by reconstituted caspases. *Proc. Natl. Acad. Sci. USA* 104: 2283–2288.
- Copela, L. A., C. F. Fernandez, R. L. Sherrer, and S. L. Wolin, 2008 Competition between the Rex1 exonuclease and the La protein affects both Trf4p-mediated RNA quality control and pre-tRNA maturation. *RNA* 14: 1214–1227.
- Espósito, G., E. Di Schiavi, C. Bergamasco, and P. Bazzicalupo, 2007 Efficient and cell specific knock-down of gene function in targeted *C. elegans* neurons. *Gene* 395: 170–176.
- Faber, P. W., J. R. Alter, M. E. MacDonald, and A. C. Hart, 1999 Polyglutamine-mediated dysfunction and apoptotic death of a *Caenorhabditis elegans* sensory neuron. *Proc. Natl. Acad. Sci. USA* 96: 179–184.
- Faber, P. W., C. Voisine, D. C. King, E. A. Bates, and A. C. Hart, 2002 Glutamine/proline-rich PQE-1 proteins protect *Caenorhabditis elegans* neurons from huntingtin polyglutamine neurotoxicity. *Proc. Natl. Acad. Sci. USA* 99: 17131–17136.
- Ferrell, J. E., 2002 Self-perpetuating states in signal transduction: positive feedback, double-negative feedback and bistability. *Curr. Opin. Cell Biol.* 14: 140–148.
- Freyd, G., S. K. Kim, and H. R. Horvitz, 1990 Novel cysteine-rich motif and homeodomain in the product of the *Caenorhabditis elegans* cell lineage gene *lin-11*. *Nature* 344: 876–879.
- Frøkjær-Jensen, C., M. W. Davis, C. E. Hopkins, B. J. Newman, J. M. Thummel *et al.*, 2008 Single-copy insertion of transgenes in *Caenorhabditis elegans*. *Nat. Genet.* 40: 1375–1383.
- Goldsmith, A. D., S. Sarin, S. Lockery, and O. Hobert, 2010 Developmental control of lateralized neuron size in the nematode *Caenorhabditis elegans*. *Neural Dev.* 5: 33.
- Hobert, O., T. D’Alberti, Y. Liu, and G. Ruvkun, 1998 Control of neural development and function in a thermoregulatory network by the LIM homeobox gene *lin-11*. *J. Neurosci.* 18: 2084–2096.
- Hoogewijs, D., K. Houthoofd, F. Matthijssens, J. Vandesompele, and J. R. Vanfleteren, 2008 Selection and validation of a set of reliable reference genes for quantitative sod gene expression analysis in *C. elegans*. *BMC Mol. Biol.* 9: 9.
- Hsieh, J., and A. Fire, 2000 Recognition and silencing of repeated DNA. *Annu. Rev. Genet.* 34: 187–204.
- Hsieh, J., J. Liu, S. A. Kostas, C. Chang, P. W. Sternberg *et al.*, 1999 The RING finger/B-box factor TAM-1 and a retinoblastoma-like protein LIN-35 modulate context-dependent gene silencing in *Caenorhabditis elegans*. *Genes Dev.* 13: 2958–2970.
- Iino, Y., and K. Yoshida, 2009 Parallel use of two behavioral mechanisms for chemotaxis in *Caenorhabditis elegans*. *J. Neurosci.* 29: 5370–5380.
- Ikemura, T., 1985 Codon usage and tRNA content in unicellular and multicellular organisms. *Mol. Biol. Evol.* 2: 13–34.
- Kelly, W. G., S. Xu, M. K. Montgomery, and A. Fire, 1997 Distinct requirements for somatic and germline expression of a generally expressed *Caenorhabditis elegans* gene. *Genetics* 146: 227–238.
- Kudla, G., A. W. Murray, D. Tollervey, and J. B. Plotkin, 2009 Coding-sequence determinants of gene expression in *Escherichia coli*. *Science* 324: 255–258.
- Le Hir, H., A. Nott, and M. J. Moore, 2003 How introns influence and enhance eukaryotic gene expression. *Trends Biochem. Sci.* 28: 215–220.
- Lee, L. W., H. W. Lo, and S. J. Lo, 2010 Vectors for co-expression of two genes in *Caenorhabditis elegans*. *Gene* 455: 16–21.
- Matsuki, M., H. Kunitomo, and Y. Iino, 2006 Galpha regulates olfactory adaptation by antagonizing Galpha-DAG signaling in *Caenorhabditis elegans*. *Proc. Natl. Acad. Sci. USA* 103: 1112–1117.
- Matz, M. V., A. F. Fradkov, Y. A. Labas, A. P. Savitsky, A. G. Zaráisky *et al.*, 1999 Fluorescent proteins from nonbioluminescent Anthozoa species. *Nat. Biotechnol.* 17: 969–973.
- Mello, C. C., J. M. Kramer, D. Stinchcomb, and V. Ambros, 1991 Efficient gene transfer in *C. elegans*: extrachromosomal maintenance and integration of transforming sequences. *EMBO J.* 10: 3959–3970.
- Mettetal, J. T., D. Muzzey, J. M. Pedraza, E. M. Ozbudak, and A. van Oudenaarden, 2006 Predicting stochastic gene expression dynamics in single cells. *Proc. Natl. Acad. Sci. USA* 103: 7304–7309.
- Mignone, F., C. Gissi, S. Liuni, and G. Pesole, 2002 Untranslated regions of mRNAs. *Genome Biol* 3: REVIEWS0004.
- Miyawaki, A., J. Llopis, R. Heim, J. M. McCaffery, J. A. Adams *et al.*, 1997 Fluorescent indicators for Ca<sup>2+</sup> based on green fluorescent proteins and calmodulin. *Nature* 388: 882–887.
- Mori, I., and Y. Ohshima, 1995 Neural regulation of thermotaxis in *Caenorhabditis elegans*. *Nature* 376: 344–348.
- Nagel, G., M. Brauner, J. F. Liewald, N. Adeishvili, E. Bamberg *et al.*, 2005 Light activation of channelrhodopsin-2 in excitable cells of *Caenorhabditis elegans* triggers rapid behavioral responses. *Curr. Biol.* 15: 2279–2284.
- Nagai, T., K. Ibata, E. S. Park, M. Kubota, K. Mikoshiba *et al.*, 2002 A variant of yellow fluorescent protein with fast and efficient maturation for cell-biological applications. *Nat. Biotechnol.* 20: 87–90.
- Nakai, J., M. Ohkura, and K. Imoto, 2001 A high signal-to-noise Ca<sup>2+</sup> probe composed of a single green fluorescent protein. *Nat. Biotechnol.* 19: 137–141.
- Ozanick, S. G., X. Wang, M. Costanzo, R. L. Brost, C. Boone *et al.*, 2009 Rex1p deficiency leads to accumulation of precursor initiator tRNA<sup>Met</sup> and polyadenylation of substrate RNAs in *Saccharomyces cerevisiae*. *Nucleic Acids Res.* 37: 298–308.
- Ozbudak, E. M., M. Thattai, H. N. Lim, B. I. Shraiman, and A. Van Oudenaarden, 2004 Multistability in the lactose utilization network of *Escherichia coli*. *Nature* 427: 737–740.
- Stinchcomb, D. T., J. E. Shaw, S. H. Carr, and D. Hirsh, 1985 Extrachromosomal DNA transformation of *Caenorhabditis elegans*. *Mol. Cell. Biol.* 5: 3484–3496.
- Troemel, E. R., J. H. Chou, N. D. Dwyer, H. A. Colbert, and C. I. Bargmann, 1995 Divergent seven transmembrane receptors are candidate chemosensory receptors in *C. elegans*. *Cell* 83: 207–218.
- Tseng, R. J., K. R. Armstrong, X. Wang, and H. M. Chamberlin, 2007 The bromodomain protein LEX-1 acts with TAM-1 to modulate gene expression in *C. elegans*. *Mol. Genet. Genomics* 278: 507–518.

- White, J. G., H. R. Horvitz, and J. E. Sulston, 1982 Neuron differentiation in cell lineage mutants of *Caenorhabditis elegans*. *Nature* 297: 584–587.
- Wicks, S. R., R. T. Yeh, W. R. Gish, R. H. Waterston, and R. H. Plasterk, 2001 Rapid gene mapping in *Caenorhabditis elegans* using a high density polymorphism map. *Nat. Genet.* 28: 160–164.
- Williams, A. J., and H. L. Paulson, 2008 Polyglutamine neurodegeneration: protein misfolding revisited. *Trends Neurosci.* 31: 521–528.
- Yamada, K., T. Hirotsu, M. Matsuki, R. Butcher, M. Tomioka *et al.*, 2010 Olfactory plasticity is regulated by pheromonal signaling in *Caenorhabditis elegans*. *Science* 329: 1647–1650.
- Zhang, F., L. P. Wang, M. Brauner, J. F. Liewald, K. Kay *et al.*, 2007 Multimodal fast optical interrogation of neural circuitry. *Nature* 446: 633–639.

*Communicating editor: Brenda J. Andrews*